The $\gamma p \to \phi\eta' p$ reaction in an effective Lagrangian model

Shao-Fei Chen and Bo-Chao Liu*
School of Physics, Xi'an Jiaotong University, Xi'an, Shaanxi 710049, China

(Received 12 February 2020; accepted 17 July 2020; published 10 August 2020)

In this work, we investigate the production of nucleon resonances in the $\gamma p \to \phi\eta' p$ reaction within an effective Lagrangian approach and isobar model. We first discuss the possible roles of the $N(1895)$, $N(1900)$, $N(2100)$, and $N(2120)$ productions in this reaction. By considering the π, η, and η' exchanges between the initial γ and proton, we find that the excitation of the $N(1895)$ in the intermediate state gives the most important contribution near the threshold. The dominant role of the $N(1895)$ is mainly attributed to its large coupling to the $N\eta$ and $N\eta'$ channels. Additionally, we also discuss the possibility of looking for a new nucleon resonance proposed in some recent works. We find that if this resonance indeed exists it should also show signals in the present reaction. Thus the present reaction offers the opportunities to study the properties of the $N(1895)$ and test the existence of the proposed new nucleon resonance.

DOI: 10.1103/PhysRevC.102.025202

I. INTRODUCTION

The study of the spectrum of nucleon resonances is a primary topic in light hadron physics. In recent years, much effort and achievement has been made in this field [1]. Among various channels that nucleon resonances can decay to, the $N\eta'$ channel is very interesting since it is a pure $I = \frac{1}{2}$ channel and thus is relatively clean for studying nucleon resonance. Besides, because the threshold energy of the $N\eta'$ channel is about 1.9 GeV, it is suitable for investigating the nucleon resonances in this region (the so-called fourth resonance region in the literature), of which resonances our knowledge is still relatively poor. Furthermore, the significant $s\bar{s}$ component of η' also makes this channel a potentially good place to look for the so-called missing resonance, which means the resonances predicted by quark models but not found by experiments. It is logical to expect that some of the missing resonances may have relatively large coupling to $N\eta'$ and thus can be found in this channel. Even with these merits, the $N\eta'$ channel was relatively poorly studied in previous works. It was not until very recently that the $N\eta'$ channel was included in the summary table of nucleon resonances in the Particle Data Group (PDG) book [2]. This is mainly attributed to the relatively low production rate of the $N\eta'$ channel and the statistics of previous experimental data was rather low. However, such situations have been changed in recent years. The high-precise data of the photon induced η' production process have become available [3–8], which offer a very good basis to study the properties of nucleon resonances in the $N\eta'$ channel.

The new data have simulated a series of theoretical works on analyzing these data. In Ref. [9], a chiral quark-model approach is adopted to study the $\gamma N \to \eta' N$ reactions. In their model, the $N(1535)\frac{1}{2}^-$, $N(2080)\frac{5}{2}^+$ and background contributions are essential for describing the data. In a later work [10], the authors made a combined analysis of the $\gamma N \to \eta' N$, $NN \to NN\eta'$, and $\pi N \to \eta' N$ reactions. They found that by taking into account four resonances, i.e., $N(1720)\frac{3}{2}^+$, $N(1925)\frac{1}{2}^-$, $N(2130)\frac{1}{2}^+$, and $N(2050)\frac{3}{2}^+$, they could reproduce all these data well. Note that, in the two works mentioned above, polarization data were not available then and were not considered in their works. The new experimental data including the precise angular distributions [6] and beam asymmetry [7,8] are considered in some more recent works. In Ref. [11], partial wave analysis of the $\gamma p \to \eta' p$ reaction was performed by also including the new data. Their conclusion is that the $N(1895)\frac{1}{2}^-$, $N(1900)\frac{3}{2}^+$, $N(2100)\frac{1}{2}^+$, and $N(2120)\frac{3}{2}^-$ are most important for describing this reaction. Based on an undated EtaMAID2018 model [12], it was, however, argued that $N(1895)\frac{1}{2}^-$, $N(1880)\frac{1}{2}^+$, $N(2100)\frac{1}{2}^+$, $N(2000)\frac{5}{2}^-$, and $N(1900)\frac{7}{2}^+$ are most important to describe the data. In another analysis of this reaction based on isobar model [13], the contributions of various nucleon resonances are considered. However, the needed resonances for describing the data are quite different from other works mentioned above. Very interestingly, in Ref. [14] a very narrow resonance $N(1900)\frac{3}{2}^-$ with $\Gamma < 3$ MeV was argued in the $\gamma p \to \eta' p$ reaction. This resonance is clearly unexpected and was not observed before. In Ref. [12], it was confirmed that a new nucleon resonance might exist but with different quantum numbers, i.e., $J^P = \frac{1}{2}^-$. Obviously, the status of relevant studies are still unsatisfied and further studies are still needed.

The main purpose of this work is to show that the $\gamma p \to p\phi\eta'$ reaction is an alternatively good place to study resonances having large coupling to $N\eta'$. As discussed in Refs. [15,16], the $\gamma p \to \phi N^*$ process is suitable for studying nucleon resonances having strong coupling to channels with significant strange component. This attribute can be illustrated by the Feynman diagrams shown in Fig. 1. Since vector meson

*liubc@xjtu.edu.cn

 ©2020 American Physical Society

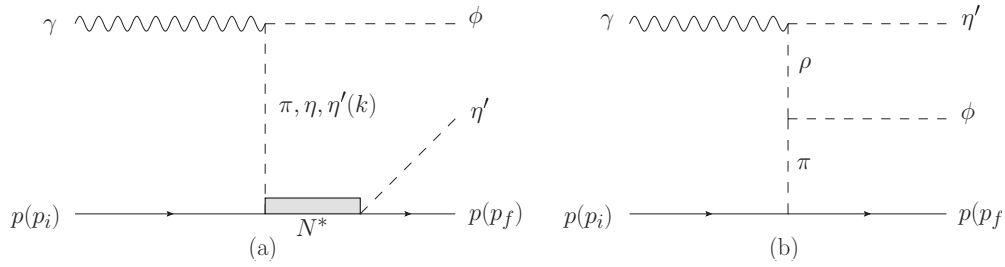

FIG. 1. Feynman diagrams for the reaction $\gamma p \to \phi\eta' p$.

exchange is forbidden by the law of C parity conservation and π exchange is suppressed due to the small $\gamma\phi\pi$ coupling, the nucleon resonances, which have large coupling to $N\eta$ or $N\eta'$ are expected to play more important role in this process. Furthermore if the N^* decays to $N\eta'$ channel, it is natural to expect that the contributions of nucleon resonances, which have large coupling to $N\eta'$ should be enhanced and thus offer a good place to investigate them. To estimate the cross sections of this reaction, we consider the nucleon resonances having significant coupling to $N\eta'$ as suggested by PDG and use the PDG averaged values of branch ratios to obtain the relevant coupling constants. The contributions of various nucleon resonances are calculated and the model predictions for the angular distribution and invariant mass spectrum are presented. Furthermore, we also discuss the possible role of the new nucleon resonance suggested in recent works [12,14]. These predictions can be tested by future experiments and help to verify our knowledge about the relevant nucleon resonances.

This paper is organized as follows. In Sec. II, the theoretical framework and amplitudes are presented for the reaction $\gamma p \to \phi\eta' p$. In Sec. III, the numerical results are presented with discussions. Finally, the paper ends with a short summary in Sec. IV.

II. FORMALISM AND INGREDIENTS

In this work, we study the $\gamma p \to \phi\eta' p$ reaction within an effective Lagrangian approach and isobar model. We assume that this reaction mainly proceeds through the excitation of nucleon resonances in the intermediate states and background term.[1] The corresponding Feynman diagrams are depicted in Fig. 1. Here we consider the contributions from the $N(1895)\frac{1}{2}^-$, $N(1900)\frac{3}{2}^+$, $N(2100)\frac{1}{2}^+$, and $N(2120)\frac{3}{2}^-$, which have relatively large coupling to the $N\eta'$ channel [2]. The parameters of these nucleon resonances are taken from the PDG book and shown in Table I. To evaluate the Feynman diagrams, the Lagrangians for various vertices are needed. The Lagrangian densities for the vertices involving nucleon resonances are [10,15]

$$\mathcal{L}^{1/2^-}_{PNN^*} = ig_{PNN^*}\bar{N}^* PN + \text{H.c.} \tag{1}$$

$$\mathcal{L}^{1/2^+}_{PNN^*} = -\frac{g_{PNN^*}}{m_N + m^*_N}\bar{N}^*\gamma_5\gamma_\mu\partial^\mu PN + \text{H.c.} \tag{2}$$

$$\mathcal{L}^{3/2^+}_{PNN^*} = -\frac{g_{PNN^*}}{m_P}\bar{N}^*_\mu\partial^\mu PN + \text{H.c.} \tag{3}$$

$$\mathcal{L}^{3/2^-}_{PNN^*} = -\frac{g_{PNN^*}}{m_P}\bar{N}^*_\mu\partial^\mu P\gamma_5 N + \text{H.c.}, \tag{4}$$

where N^*, N, and P denote the fields of the nucleon resonance, nucleon, and $\eta(\eta')$, respectively. The coupling constants in the Lagrangians can be evaluated through the corresponding partial decay width (see Appendix) and the obtained values are listed in Table I. Other needed Lagrangian densities are

$$\mathcal{L}_{\gamma\phi P} = \frac{e}{m_\phi}g_{\gamma\phi P}\varepsilon^{\mu\nu\alpha\beta}\partial_\mu\phi_\nu\partial_\alpha A_\beta P \tag{5}$$

$$\mathcal{L}_{\gamma\eta'\rho} = \frac{e}{m_{\eta'}}g_{\gamma\eta'\rho}\varepsilon^{\mu\nu\alpha\beta}\partial_\mu\rho_\nu\partial_\alpha A_\beta\eta' \tag{6}$$

$$\mathcal{L}_{\rho\pi\phi} = \frac{e}{m_\phi}g_{\rho\pi\phi}\varepsilon^{\mu\nu\alpha\beta}\partial_\mu\phi_\nu\partial_\alpha\rho_\beta\pi \tag{7}$$

$$\mathcal{L}_{NN\pi} = -\frac{g_{NN\pi}}{2m_N}\bar{N}\gamma_5\gamma_\mu\vec{\tau}\cdot\partial^\mu\vec{\pi}N, \tag{8}$$

where π, ϕ, and A represent the quantum fields of the π, ϕ, and photon. For coupling constants, we have $e = \sqrt{4\pi/137}$ and $g_{NN\pi} = 13.45$ [20,21]. Other coupling constants are also obtained from the partial decay widths and listed in Table I. Note that through the partial decay width only the magnitude of the coupling constant can be determined. Therefore, we have chosen a positive sign for the coupling constants in the calculations. The possible effects due to the relative phases are discussed in the content concerning the interference effects in Sec. III.

The propagators for the exchanged pseudoscalar meson P($=\pi$, η, η') and vector meson ρ are

$$G_P(q) = \frac{i}{q^2 - m_P^2},$$

$$G^{\mu\nu}_\rho(q) = -\frac{i(g^{\mu\nu} - q^\mu q^\nu/q^2)}{q^2 - m_\rho^2}.$$

[1]Very recently, an enhancement in the $\phi\eta'$ mass spectrum in $J/\psi \to \phi\eta\eta'$ was observed [17]. In principle, if this resonance (named as X) indeed exists it may also contribute to the reaction under study. To evaluate its contribution, the X-γ-meson coupling is needed, for which we still do not know. While, it is logical to expect X may have relatively large coupling to $\gamma\eta$ or $\gamma\eta'$ channels, and then the η/η' exchange should be important for the excitation of X in this reaction. However, due to the small couplings of $NN\eta$ or $NN\eta'$ vertices [18,19], we thus ignore its contribution.

TABLE I. The coupling constants adopted in this work.

State	Math/Width (MeV)	Decay channel	Adopt branching ratio	$g^2/4\pi$[a]
ϕ	1019/4.25	$\pi\gamma$	1.3×10^{-3}	1.60×10^{-3}
		$\eta\gamma$	1.3 %	3.97×10^{-2}
		$\eta'\gamma$	6.22×10^{-5}	4.31×10^{-2}
		$\rho\pi$	15 %	3.55
$N(1895)$	1895/120	$N\eta$	25 %	4.85×10^{-2}
		$N\eta'$	20 %	0.41*
		$N\pi$	10 %	5.07×10^{-3}
$N(2100)$	2100/260	$N\eta'$	8 %	0.94
		$N\pi$	12 %	8.26×10^{-2}
$N(1900)$	1920/200	$N\eta$	8 %	6.40×10^{-2}
		$N\eta'$	6 %	3.21*
		$N\pi$	10 %	8.72×10^{-4}
$N(2120)$	2120/300	$N\eta'$	4 %	5.81
		$N\pi$	10 %	5.89×10^{-3}
η'	958/0.23	$\gamma\rho$	29 %	0.15

[a]The values of $g^2/4\pi$ with an asterisk are obtained by Eq. (A6). Others are calculated from Eqs. (A1)–(A5).

The corresponding propagators for nucleon resonances with $J = \frac{1}{2}$ and $\frac{3}{2}$ are

$$G_{\frac{1}{2}}(q) = \frac{i(\not{q} + M_{N^*})}{q^2 - M_{N^*}^2 + iM_{N^*}\Gamma_{N^*}},$$
$$G^{\mu\nu}_{\frac{3}{2}}(q) = \frac{i(\not{q} + M_{N^*})P^{\mu\nu}(q)}{q^2 - M_{N^*}^2 + iM_{N^*}\Gamma_{N^*}}$$

with

$$P^{\mu\nu}(q) = -g^{\mu\nu} + \frac{1}{3}\gamma^\mu\gamma^\nu + \frac{1}{3M_{N^*}}(\gamma^\mu q^\nu - \gamma^\nu q^\mu) + \frac{2}{3M_{N^*}^2}q^\mu q^\nu.$$

As hadrons are not pointlike particles, we have taken into account their internal structure and possible off-shell effects by introducing form factors. For the baryon exchange diagrams, we use the form factor [22,23]

$$F_B(q_{ex}, m_{ex}) = \frac{\Lambda_B^4}{\Lambda_B^4 + \left(q_{ex}^2 - m_{ex}^2\right)^2}. \quad (9)$$

For meson exchange diagrams, we take the form factor employed in Refs. [20,24]

$$F_M(q_{ex}, m_{ex}) = \left(\frac{\Lambda_M^2 - m_{ex}^2}{\Lambda_M^2 - q_{ex}^2}\right)^2. \quad (10)$$

While, the form factor for the $\gamma\rho\eta'$ vertex is adopted as [25]

$$F_V(q_{ex}, m_{ex}) = \left(\frac{\Lambda_V^2}{\Lambda_V^2 - q_{ex}^2}\right)^2. \quad (11)$$

The q_{ex} and m_{ex} are the four-momentum and mass of the exchanged particle. In a phenomenological approach, the cutoff parameters can only be determined by fitting to the experimental data. Here we adopt the values that are determined by studying other reactions. To be concrete, we take $\Lambda_\pi = \Lambda_\eta = 1.3$ GeV and $\Lambda_\rho = 1.2$ GeV for the corresponding meson exchanges [20,26] and $\Lambda_N* = 2.0$ GeV for baryon exchanges [15]. The cutoff parameter $\Lambda_{\eta'}$ for the η' meson exchange is not well determined in previous works. To evaluate its value, we adopt a popular parametrization of the cutoff parameter, which can be presented as

$$\Lambda = m_{ex} + \alpha\Lambda_{QCD}. \quad (12)$$

The typical value for Λ_{QCD} is about 300 MeV [2]. The free parameter α cannot be calculated from first principles. In literatures, the α varies in a range from 1.0–2.0 [27]. In this work, we will employ $\alpha = 1.0$ in the calculations and thus the value of $\Lambda_{\eta'}$ is taken as $\Lambda_{\eta'} = 1.26$ GeV. The uncertainties due to this parameter will be discussion in Sec. III.

With all the ingredients given above, the amplitudes can be constructed and the obtained amplitudes are as follows:

$$M_{N^*_{\frac{1}{2}^-}} = -\frac{ie}{m_\phi}g_{\phi\gamma P}g_{NN^*P}g_{\eta' N^* N} \times \bar{u}(p_f, m_p)G_{\frac{1}{2}}(p_{N^*})u(p_i, m_p)G_0(k) \times \varepsilon_{\mu\nu\alpha\beta}p_\phi^\mu\varepsilon^{*\nu}(p_\phi, s_\phi)p_\gamma^\alpha\varepsilon^\beta(p_\gamma, s_\gamma) \times F_B(p_{N^*}, m_{N^*})F_M(k, m_P) \quad (13)$$

$$M_{N^*_{\frac{1}{2}^+}} = \frac{ie}{m_\phi}\frac{g_{\phi\gamma P}g_{NN^*P}g_{\eta' N^* N}}{(m_p + m_{N^*})^2} \times \bar{u}(p_f, m_p)\not{p}_{\eta'}\gamma_5 G_{\frac{1}{2}}(p_{N^*})\gamma_5\not{k}u(p_i, m_p) \times G_0(k)\varepsilon_{\mu\nu\alpha\beta}p_\phi^\mu\varepsilon^{*\nu}(p_\phi, s_\phi)p_\gamma^\alpha\varepsilon^\beta(p_\gamma, s_\gamma) \times F_B(p_{N^*}, m_{N^*})F_M(k, m_P) \quad (14)$$

$$M_{N^*_{\frac{3}{2}^+}} = \frac{ie}{m_\phi}\frac{g_{\phi\gamma P}g_{NN^*P}g_{\eta' N^* N}}{m_P m_{\eta'}} \times \bar{u}(p_f, m_p)p_{\eta'\rho}G^{\rho\sigma}_{\frac{3}{2}}(p_{N^*})k_\sigma u(p_i, m_p) \times G_0(k)\varepsilon_{\mu\nu\alpha\beta}p_\phi^\mu\varepsilon^{*\nu}(p_\phi, s_\phi)p_\gamma^\alpha\varepsilon^\beta(p_\gamma, s_\gamma) \times F_B(p_{N^*}, m_{N^*})F_M(k, m_P) \quad (15)$$

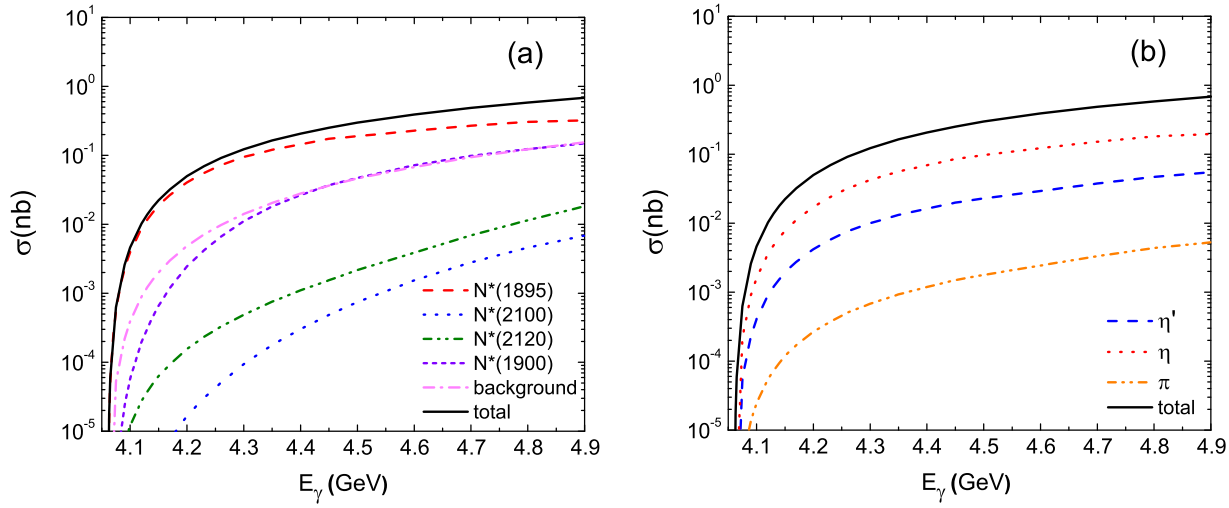

FIG. 2. Total cross sections for the $\gamma p \to \phi\eta' p$ reaction as a function of the beam energy E_γ with individual contributions from (a) various nucleon resonance and background term and (b) contributions from various meson exchanges.

$$M_{N^*_{\frac{3}{2}^-}} = \frac{ie}{m_\phi}\frac{g_{\phi\gamma P}g_{NN^*P}g_{\eta' N^* N}}{m_\eta m_{\eta'}} \times\bar{u}(p_f,m_p)\gamma_5 p\!\!\!/_{\eta'}\rho G^{\rho\sigma}_{\frac{3}{2}}(p_{N^*})k_\sigma\gamma_5 u(p_i,m_p) \times G_0(k)\varepsilon_{\mu\nu\alpha\beta}p^\mu_\phi\varepsilon^{*\nu}(p_\phi,s_\phi)p^\alpha_\gamma\varepsilon^\beta(p_\gamma,s_\gamma) \times F_B(p_{N^*},m_{N^*})F_M(k,m_P) \quad (16)$$

$$M_{bg} = \frac{e^2}{2m_p}\frac{g_{\phi\rho\pi}g_{\eta'\rho\gamma}g_{\pi NN}}{m_\phi m'_\eta}\varepsilon_{\mu\nu\alpha\beta}p^\mu_\phi\varepsilon^{*\nu}(p_\phi,s_\phi)p^\alpha_\rho \times G_1^{\beta b}(p_\rho)\varepsilon_{abcd}p^a_\rho p^c_\gamma\varepsilon^d(p_\gamma,s_\gamma)G_0(p_\pi) \times\bar{u}(p_f,m_p)\gamma_5\ p\!\!\!/_\pi u(p_i,m_p) \times F_M(p_\pi,m_\pi)F_V(p_\rho,m_\rho), \quad (17)$$

where p_i and p_f represent the four-momentum of the initial and final proton, respectively. P denotes the exchanged pseudoscalar meson η, η', or π.

The differential and total cross sections for this reaction can be calculated through

$$d\sigma = \frac{1}{8}\frac{m_N}{(2\pi)^5(p_i\cdot p_\gamma)}\sum_{\lambda_\phi\lambda_\gamma\lambda_i\lambda_f}|\mathcal{M}|^2\frac{m_N d^3p_f}{E_f}\frac{d^3p_\phi}{2E_\phi}\frac{d^3p_{\eta'}}{2E_{\eta'}} \times\ \delta^4(p_i+p_\gamma-p_f-p_\phi-p_{\eta'}), \quad (18)$$

where λ_ϕ, λ_γ, λ_i, and λ_f are the helicities of the ϕ meson, photon, initial, and final protons, respectively. $\mathcal{M}$ is the corresponding full amplitude of this reaction.

III. RESULTS AND DISCUSSION

In this section, we present the calculated results for the $\gamma p \to \phi\eta' p$ reaction based on the model described above. The results for the total cross sections from threshold up to 4.9 GeV, together with the contributions from individual nucleon resonances and various meson exchanges, are plotted in Fig. 2. As shown in Fig. 2(a), it is found that the $N(1895)$ gives the most important contribution in this reaction. As close to the threshold, its contribution becomes dominant. The dominant role of the $N(1895)$ is mainly attributed to its large couplings to the $N\eta$ and $N\eta'$ channels and the s-wave nature of its coupling to $N\eta'$. Other resonances and background terms only play minor roles in this reaction. With the beam energy increasing, their contributions will become more important. The solid line represents the sum of the contributions from individual nucleon resonances and background term. The interference effects among the individual contributions rely on the relative phases, which are not well determined in our model. However, to have a feeling about the uncertainties due to the interference effects, we have tried various relative phases among the amplitudes of the nucleon resonances and the background term and found the change of the total cross sections is within 25%. At the near threshold region, the interference effects become negligible because the production of the $N(1895)$ dominates this reaction. Due to the dominant role of the $N(1895)$ at the near threshold region, this reaction may offer a nice place to investigate its properties. The individual contributions of π, η, and η' exchanges are plotted in Fig. 2(b). It shows that the η exchange plays the most important role for the excitation of the nucleon resonances in this reaction. While, the π exchange only plays a relatively unimportant role here.

As mentioned in Sec. I, the study of the present reaction provides a good supplement to the studies of the nucleon resonances in the $\gamma p \to p\eta'$ reaction. In the very recent works [12,14], the authors argued that there were evidences of a new nucleon resonance having extremely small width in the $\gamma p \to p\eta'$ reaction near threshold. Up to now, the existence of this resonance is still not well identified. It is then valuable to discuss the possibility of looking for the narrow resonance in the present reaction. Since till now the signal of the narrow resonance was only found in the $\gamma p \to p\eta'$ reaction, it is natural to expect that the narrow resonance has a relatively large coupling to the $N\eta'$ channel and thus should also be present in the reaction under study. Compared to the $\gamma p \to p\eta'$ reaction, the present reaction is suitable to look for this

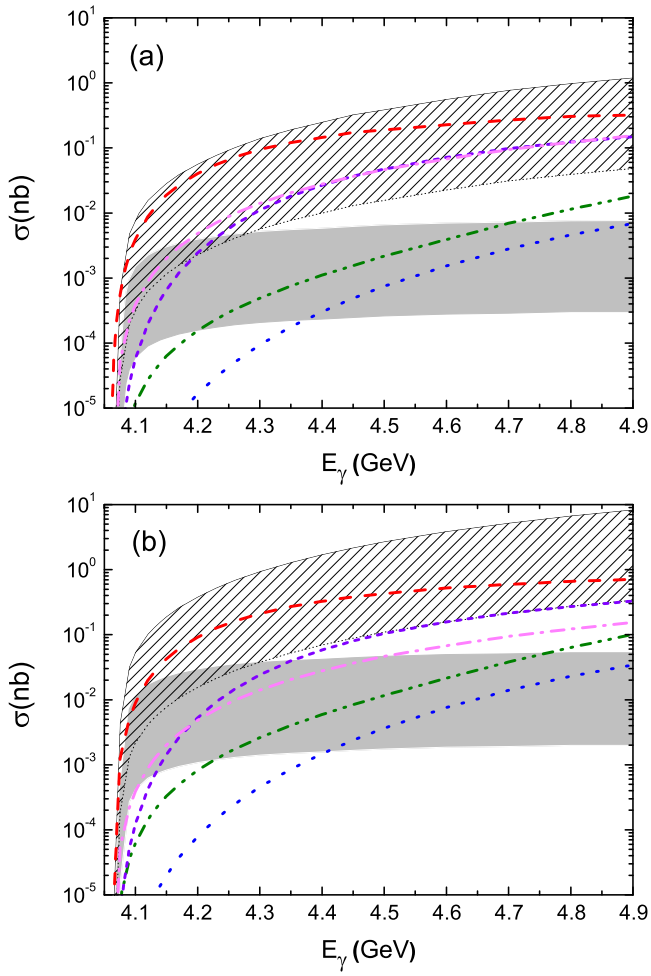

FIG. 3. Total cross sections for the $\gamma p \to \phi\eta' p$ reaction as a function of the beam energy E_γ with taking (a) $\alpha = 1.0$ and (b) $\alpha = 2.0$. The gray and slashed bands represents the uncertainties due to the branching ratio of $N^* \to N\eta'$ varying from 10%–50% for the $\frac{1}{2}^-$ and $\frac{3}{2}^-$ assignments for the new resonance respectively. Other lines have the same meanings as Fig. 2(a).

new resonance since the γ-ϕ-meson vertex enhances the η and η' exchange contributions and thus may amplify the signal of the new resonance. As suggested in Refs. [12,14], the mass, width, and J^P quantum numbers of this new resonance may be $M = 1900$ MeV, $\Gamma = 3$ MeV, and $J^P = \frac{3}{2}^-$(denoted as $N^*_{\frac{3}{2}^-}$ hereafter) or $M = 1902.6$ MeV, $\Gamma = 2.1$ MeV, and $J^P = \frac{1}{2}^-$(denoted as $N^*_{\frac{1}{2}^-}$ hereafter).[2] In the following, we will consider both these two assignments and examine their possible contributions individually. To obtain the coupling constants of the $N^*_{\frac{3}{2}^-}N\eta'$ or $N^*_{\frac{1}{2}^-}N\eta'$ vertices, we have assumed that the branch ratio of the new resonance decaying to $N\eta'$, i.e., $Br(N^* \to N\eta')$, lies within 10%–50%. Then, the cross sections by only considering the η' exchange can be calculated and are shown in Fig. 3(a). To estimate the uncertainties due to the parameter α, here we also show the results for $\alpha = 2.0$ [Fig. 3(b)]. By taking $\alpha = 2.0$, the cutoff parameter $\Lambda_{\eta'}$ is then taken as 1.56 GeV, which will enhance the η' exchange contribution. It is found that the η' exchange can be enhanced by a factor of about 7 due to this change. While, the relative roles of the nucleon resonances are basically unchanged. The bands in the figures reflect the uncertainties of the contribution of the $N^*_{\frac{3}{2}^-}$ or $N^*_{\frac{1}{2}^-}$ due to the $Br(N^* \to N\eta')$ varying from 10%–50%. As can be seen from the figure, the obtained cross sections for the $N^*_{\frac{3}{2}^-}$ production is larger than those for the $N^*_{\frac{1}{2}^-}$ case even though a same value for the $Br(N^* \to N\eta')$ is adopted. The enhancement for the $N^*_{\frac{3}{2}^-}$ production can be understood in the following way. At the nucleon resonance production vertex, the vertex function of the $N^*N\eta(\eta')$ vertex is roughly proportional to p^L_{th} at the near threshold region, where p_{th} is the magnitude of the threshold momentum of the $\gamma p \to \phi\eta' p$ reaction in the center of mass frame and L is the relative orbital angular momentum of $N\eta'$ system in the $N^* \to N\eta'$ process. In order to produce the $\phi\eta' p$ final states, a large threshold momentum is needed, which then enhances the $N^*_{\frac{3}{2}^-}(L = 2)$ production due to the p^L_{th} factor compared to the production of the $N^*_{\frac{1}{2}^-}(L = 0)$. The trend of the cross sections at higher energies can be understood in a similar way. With taking $Br(N^* \to N\eta') = 50\%$, we find the production of the new resonance gives considerable contributions to the total cross sections for both the $N^*_{\frac{3}{2}^-}$ and $N^*_{\frac{1}{2}^-}$ cases at the near threshold region. However, with taking $Br(N^* \to N\eta') = 10\%$, the production of the new nucleon resonance will only play a minor role in this reaction. Since the knowledge of their decay branch ratios are still lacking, it is then helpful to examine their effects in the two limit cases, i.e., $Br(N^* \to N\eta') = 10\%$ or 50%.

In Fig. 4, we study the spectrum of the invariant mass $M_{p\eta'}$ with and without the contribution from the proposed new nucleon resonance.[3] In Fig. 4(a), we first study the $N^*_{\frac{3}{2}^-}$ case. To compare the results taking $Br(N^* \to N\eta') = 10\%$ or 50% and the result without considering the new resonance in one figure, we have rescaled the invariant mass distributions by multiplying a constant factor. As can be seen from the figure, if we adopt $Br(N^*_{\frac{3}{2}^-} \to N\eta') = 50\%$ the new $N^*_{\frac{3}{2}^-}$ will cause a very sharp peak in the $M_{p\eta'}$ spectrum. Even if $Br(N^*_{\frac{3}{2}^-} \to N\eta') = 10\%$ is adopted, there is still a small bump shown in the $M_{p\eta'}$ spectrum. The corresponding results for the $N^*_{\frac{1}{2}^-}$ case are shown in Fig. 4(b). In this case, we

[2]For the $J^P = \frac{3}{2}^-$ assignment, only the upper limit of the width is available, so we adopt this value in the calculations. We have checked, with adopting a smaller width such as $\Gamma = 2.1$ MeV, the main results will not change significantly. For other parameters of the resonances, we simply use the central values suggested by the references.

[3]We have checked that by taking the parameter $\alpha = 1.0$ or 2.0 the differential cross sections show similar patterns. So in the following we will only show the results with taking $\alpha = 1.0$.

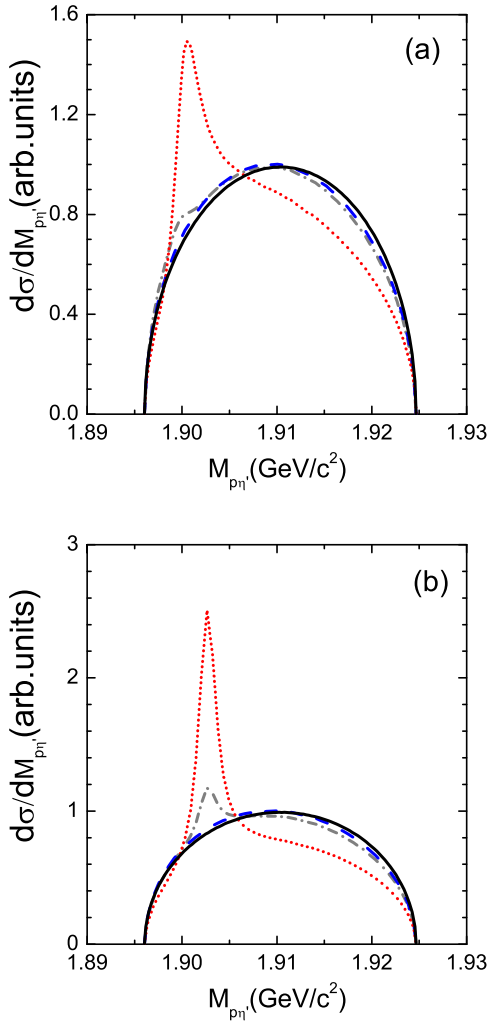

FIG. 4. Invariant mass distributions of the final $p\eta'$ pair at $E_\gamma = 4.15$ GeV for (a) the $N^*_{\frac{3}{2}^-}$ case and (b) the $N^*_{\frac{1}{2}^-}$ case. The red dotted line, the gray dash-dotted line, and the blue dashed line represent the results with taking $Br(N^*_{\frac{3}{2}^-/\frac{1}{2}^-} \to N\eta') = 50\%$, 10%, and the results without the new resonance's contribution. The black solid line stands for the pure phase space distribution.

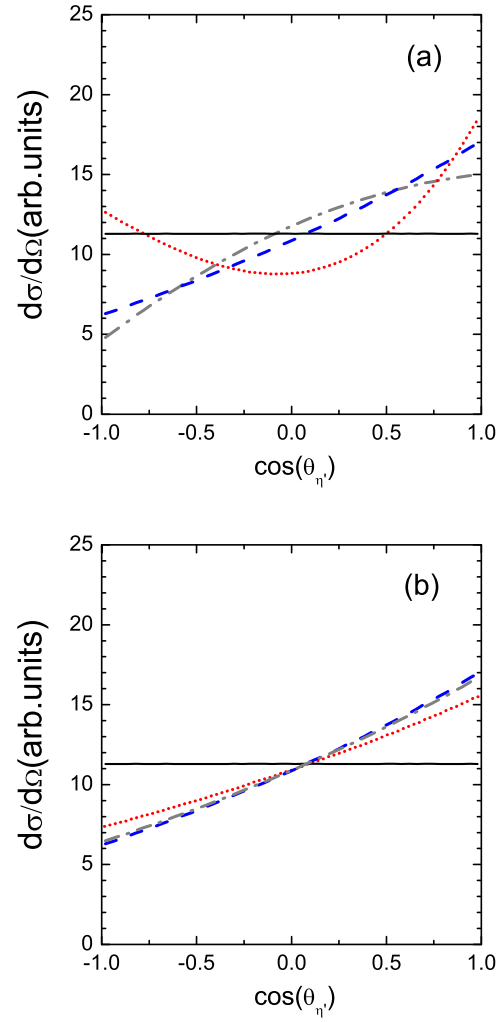

FIG. 5. Angular distribution of η' in the $p\eta'$ rest frame at $E_\gamma = 4.15$ GeV for (a) the $N^*_{\frac{3}{2}^-}$ case and (b) the $N^*_{\frac{1}{2}^-}$ case with $\theta_{\eta'}$ being the angle between the η' momentum and the beam direction. The instructions for various lines are the same as those for Fig. 4.

find the signal of the new nucleon resonance is also clearly seen. In fact, the signal of the $N^*_{\frac{1}{2}^-}$ in the invariant mass spectrum seems more pronounced than that in the $N^*_{\frac{3}{2}^-}$ case. This result may seem to conflict with naive expectations based on the corresponding total cross sections shown in Fig. 2(a). Through a more detailed study, we find the reason for this is that the interference between the $N^*_{\frac{1}{2}^-}$ and the $N(1895)\frac{1}{2}^-$ amplitudes is much stronger than the interference between the $N^*_{\frac{3}{2}^-}$ and the $N(1895)\frac{1}{2}^-$ amplitudes. Through the interference effects, the signal of the $N^*_{\frac{1}{2}^-}$ is thus amplified due to the dominance contributions of the $N(1895)\frac{1}{2}^-$. Note that in the results shown in Fig. 4 we have assumed the production amplitudes of the $N^*_{\frac{3}{2}^-}$ or $N^*_{\frac{1}{2}^-}$ have positive interference with the amplitude of the $N(1895)\frac{1}{2}^-$. If negative interference is adopted, the peak of the new resonance will be replaced by a dip structure with a similar magnitude for the $N^*_{\frac{1}{2}^-}$ case. While, such change only induces a minor effect for the $N^*_{\frac{3}{2}^-}$ case. This observation is in accordance with the conclusion that the peak of the $N^*_{\frac{1}{2}^-}$ shown in Fig. 4(b) is mainly due to the interference effects.

In Fig. 5, we study the η' angular distribution in the $p\eta'$ rest frame, which may offer clues about the quantum numbers of the new resonance. To compare the results for various cases in one figure, the differential cross sections are also rescaled to the same range. In Fig. 5(a), we study the angular distribution of the η' in the $N^*_{\frac{3}{2}^-}$ case. In this case, we find that by adopting $Br(N^*_{\frac{3}{2}^-} \to N\eta') = 50\%$ the inclusion of the $N^*_{\frac{3}{2}^-}$ can significantly change the η' angular distribution and the curvature of the angular distribution [the red dotted line in Fig. 5(a)] clearly indicates the higher partial wave contribution from the

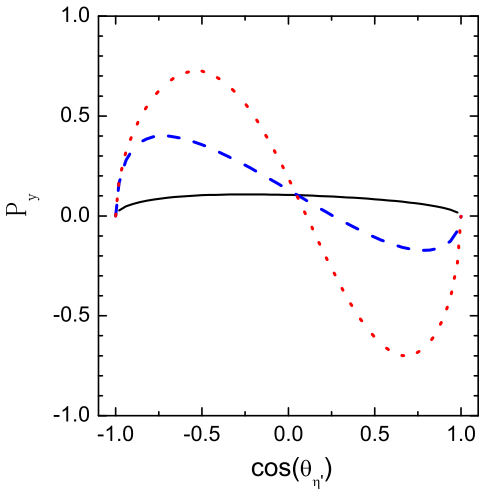

FIG. 6. Polarized target asymmetry for the $\gamma p \to \phi\eta' p$ reaction at beam energy $E_\gamma = 4.15$ GeV with $\theta_{\eta'}$ being the angle between the η' momentum and the beam direction in the $p\eta'$ rest frame. The solid line represents the results without the contribution of the new resonance. The dashed and dotted lines show the results with including the $N^*_{\frac{3}{2}^-}$ contribution by adopting $Br(N^*_{\frac{3}{2}^-} \to N\eta') = 10\%$ and 50% respectively.

new resonance. However, by adopting $Br(N^* \to N\eta') = 10\%$ the signal of the new resonance becomes insignificant. Even though it is possible to amplify its signal by making a cut on the $M_{N\eta'}$ with $M_{N\eta'} < 1.91$ GeV, this is only feasible when the statistics of data is large enough. The corresponding angular distributions with including the $N^*_{\frac{1}{2}^-}$ contribution are shown in Fig. 5(b). We find that in this case the effects due to the new resonance are not apparent. This is partly because of the relatively small production rate of the $N^*_{\frac{1}{2}^-}$ and partly because of it also being a s-wave state which make its contribution indistinguishable from the dominant contribution from the $N(1895)\frac{1}{2}^-$. Due to the different features caused by the new nucleon resonance having $J^P = \frac{1}{2}^-$ or $\frac{3}{2}^-$, we expect a combined analysis of both the invariant mass spectrum and the η' angular distribution can offer valuable information about the quantum numbers of the new nucleon resonance.

Finally, it is also interesting to discuss the possible effects of the new nucleon resonance on the polarization observables. In Refs. [12,14], it was found that the new resonance may show clear signals in the polarization observables. In our model, the nucleon resonances are excited through the exchanges of π, η, and η'. So the intermediate nucleon resonances are not sensitive to the polarization of photon beam, while it is found that the measurement of polarized target asymmetry can offer valuable information about the intermediate nucleon resonances. Following the conventions in Ref. [28], we present the predictions for the polarized target asymmetry P_y for the $N^*_{\frac{3}{2}^-}$ case in Fig. 6, where the y axis is chosen along $\vec{p}_i \times \vec{p}_f$ with $\vec{p}_i(\vec{p}_f)$ being the momentum of the initial (final) proton in the $p\eta'$ rest frame. It is found that even with taking $Br(N^*_{\frac{3}{2}^-} \to N\eta') = 10\%$ the signal of the $N^*_{\frac{3}{2}^-}$ is still clear. While for the $N^*_{\frac{1}{2}^-}$ case, we find the P_y is insensitive to the $N^*_{\frac{1}{2}^-}$'s contribution. After including the $N^*_{\frac{1}{2}^-}$'s contribution, the P_y is basically unchanged as compared to the results without the new resonance's contribution (solid line in Fig. 6). Thus the measurement of the P_y may offer the evidence for the existence of the $N^*_{\frac{3}{2}^-}$ and help us to identify its quantum numbers.

IV. SUMMARY

In summary, we have studied the $\gamma p \to \phi\eta' p$ reaction within an effective Lagrangian approach and isobar model. We investigate the possible roles of various nucleon resonances in this reaction using the PDG averaged values for their masses, widths, and decay branch ratios. Among these nucleon resonances, we find that the $N(1895)$ gives the most important contribution in this reaction. In addition, we also discuss the possibility of looking for a newly proposed nucleon resonance in the present reaction. It is found that the suggested new resonance may give significant contribution in the present reaction, which makes this reaction a suitable place for looking for this new resonance. More information about the new resonance can be obtained by studying the invariant mass spectrum, the η' angular distribution in the $p\eta'$ rest frame and the polarized target asymmetry. Therefore, the study of this reaction can provide valuable information about nucleon resonances in the intermediate states, which constitute a good supplement for relevant studies of the $\gamma p \to p\eta'$ reaction.

ACKNOWLEDGMENTS

We acknowledge the support from the National Natural Science Foundation of China under Grants No. U1832160 and No. 11375137, the Natural Science Foundation of Shaanxi Province under Grants No. 2015JQ1003 and No. 2019JM-025, and the Fundamental Research Funds for the Central Universities.

APPENDIX: COUPLING CONSTANTS

In this Appendix, we present the formulas for obtaining the coupling constants shown in Table I. In practice, the effective coupling constant can be evaluated from the corresponding partial decay width if the partial decay width is available. Using the effective Lagrangians offered in Sec. II, the expressions for the partial width for various processes can be obtained as

$$\Gamma[V \to P\gamma] = \frac{e^2 g^2_{VP\gamma}}{12\pi} \frac{|\vec{p}|^3}{m_V^2} \tag{A1}$$

$$\Gamma[\phi \to \rho_0\pi] = \frac{e^2 g^2_{\phi\rho\pi}}{12\pi} \frac{|\vec{p}|^3}{m_\phi^2} \tag{A2}$$

$$\Gamma[N^*_{1/2^\pm} \to PN] = \frac{\kappa g^2_{PNN^*}}{4\pi} \frac{(E_N \mp m_N)}{m^*_N} |\vec{p}| \tag{A3}$$

$$\Gamma[N^*_{3/2^\pm} \to PN] = \frac{\kappa g^2_{PNN^*}}{12\pi}\frac{(E_N \pm m_N)}{m^*_N m^2_P}|\vec{p}|^3 \quad \text{(A4)}$$

$$\Gamma[\eta' \to \rho\gamma] = \frac{e^2 g^2_{\eta'\rho\gamma}}{4\pi}\frac{(E_\rho + |\vec{p}|)^2|\vec{p}|^3}{m^4_{\eta'}}, \quad \text{(A5)}$$

where $|\vec{p}|$ is the magnitude of the momentum of final particles in the rest frame of the parent particle, $P(=\pi, \eta, \eta')$ and $V(=\rho, \phi)$ stand for pseudoscalar and vector mesons, and κ is the isospin coefficient taking 1 or 3 for the mesons having isospin $I = 0$ or 1, respectively.

The above formulas are suitable for resonance with mass not close to the threshold of the decay channel. In the cases for the $N(1895)$, $N(1900)$, and the proposed $N^*_{\frac{3}{2}^-}$ or $N^*_{\frac{1}{2}^-}$, they lie very close to the $N\eta'$ threshold and it is then necessary to take into account their finite widths. To include the finite width effects, we fold the expression for the width with the mass distribution of the particles as

$$\Gamma_{N^*\to NP} = -\frac{1}{\pi}\int ds \Gamma_{N^*\to NP}(\sqrt{s})\Theta(\sqrt{s} - M_P - M_N)\cdot \mathrm{Im}\left\{\frac{1}{s - M^2_{N^*} + iM_{N^*}\Gamma_{N^*}}\right\}F_B(p_{N^*}, m_{N^*}), \quad \text{(A6)}$$

where the expressions for $\Gamma_{N^*\to NP}$ are given in Eq. (A1)–Eq. (A5) with substituting $\sqrt{s}$ for m_{N^*}. The form factor taking into account the off-shell effects of the resonance [Eq. (9)] is also included for consistence.

[1] D. G. Ireland, E. Pasyuk, and I. Strakovsky, Progress Particle Nuclear Phys. **111**, 103752 (2020).
[2] M. Tanabashi *et al.* (Particle Data Group), Phys. Rev. D **98**, 030001 (2018) (and 2019 update).
[3] M. Dugger *et al.* (CLAS Collaboration), Phys. Rev. Lett. **96**, 062001 (2006); **96**, 169905(E) (2006).
[4] V. Crede *et al.* (CBELSA/TAPS Collaboration), Phys. Rev. C **80**, 055202 (2009).
[5] M. Williams *et al.* (CLAS Collaboration), Phys. Rev. C **80**, 045213 (2009).
[6] V. L. Kashevarov *et al.* (A2 Collaboration at MAMI), Phys. Rev. Lett. **118**, 212001 (2017).
[7] P. Levi Sandri *et al.*, Eur. Phys. J. A **51**, 77 (2015).
[8] P. Collins *et al.* (CLAS Collaboration), Phys. Lett. B **771**, 213 (2017).
[9] X. H. Zhong and Q. Zhao, Phys. Rev. C **84**, 065204 (2011).
[10] F. Huang, H. Haberzettl, and K. Nakayama, Phys. Rev. C **87**, 054004 (2013).
[11] A. V. Anisovich *et al.*, Phys. Lett. B **772**, 247 (2017).
[12] L. Tiator *et al.*, Eur. Phys. J. A **54**, 210 (2018).
[13] V. A. Tryasuchev, V. A. Serdyutskiy, and A. G. Kondratyeva, Phys. Atom. Nucl. **81**, 62 (2018).
[14] A. V. Anisovich *et al.*, Phys. Lett. B **785**, 626 (2018).
[15] Q. F. Lu, R. Wang, J. J. Xie, X. R. Chen, and D. M. Li, Phys. Rev. C **91**, 035204 (2015).
[16] J. Q. Fan, S. F. Chen, and B. C. Liu, Phys. Rev. C **99**, 025203 (2019).
[17] M. Ablikim *et al.* (BES Collaboration), Phys. Rev. D **99**, 112008 (2019).
[18] P. Moskal, arXiv:hep-ph/0408162.
[19] R. Machleidt, Phys. Rev. C **63**, 024001 (2001).
[20] J. J. Xie, B. S. Zou, and H. C. Chiang, Phys. Rev. C **77**, 015206 (2008).
[21] J. J. Xie, B. C. Liu, and C. S. An, Phys. Rev. C **88**, 015203 (2013).
[22] B. C. Liu and J. J. Xie, Phys. Rev. C **85**, 038201 (2012).
[23] V. Shklyar, H. Lenske, and U. Mosel, Phys. Rev. C **72**, 015210 (2005).
[24] Y. Oh, C. M. Ko, and K. Nakayama, Phys. Rev. C **77**, 045204 (2008).
[25] K. Nakayama, Y. Oh, and H. Haberzettl, J. Kor. Phys. Soc. **59**, 224 (2011).
[26] B. C. Liu and S. F. Chen, Phys. Rev. C **96**, 054001 (2017).
[27] F. Yu *et al.*, Chin. Phys. C **42**, 051001 (2018).
[28] W. Roberts and T. Oed, Phys. Rev. C **71**, 055201 (2005).